Ultramicroscopy 38 (1991) 343–347
North-Holland

ultramicroscopy

Short note

Validity of the kinematical approximation in transmission electron diffraction for surfaces, revisited

L.D. Marks, T.S. Savage, J.P. Zhang and R. Ai

Center for Surface Radiation Damage Studies, Department of Materials Science, Northwestern University, Evanston, IL 60208, USA

Received 4 July 1991

It has previously been suggested, based upon multislice calculations, that electron diffraction from a surface reconstruction can be interpreted kinematically with a pseudo-kinematical condition setup for the underlying crystal. These calculations were carried out under conditions where the numerical multislice integration would not have fully converged. The intention of this note is to provide direct experimental evidence from the boron-doped Si(111)$\sqrt{3} \times \sqrt{3}$ R30° surface that the kinematical assertion is valid.

1. Introduction

One of the most attractive ways of approaching a surface reconstruction structure for an electron microscopist is via the use of electron diffraction. Particularly if the surface diffraction spots can be interpreted kinematically, as has been suggested by Spence [1] and Tanishiro and Takanayagi [2], one can generate a surface Patterson function [3,4]. The logic behind a kinematical interpretation, if the bulk diffraction is also kinematical, is straightforward – if all of the surface diffraction spots are in a kinematical condition then to a good approximation double diffraction of them by the underlying substrate will be small for the top surface, and double diffraction of the bulk spots by the bottom surface reconstruction similarly small.

In an attempt to establish this point, in a recent paper [2] multislice simulations were performed of the Si(111) 7×7 surface using the DAS model [3,4] and detailed numerical calculations of the *R*-factor of the surface diffraction spots calculated relative to the kinematical intensities. This work appeared to demonstrate the validity of the kinematical interpretation. We have recently been working with boron-doped silicon (111), and observed the metastable (for this material) 7×7 reconstruction in conventional 2-beam (220) dark-field imaging, which implied that there may be long-range strains from the screw dislocations in the DAS structure. One of the first steps in a theoretical analysis of such image contrast is to try and reproduce existing calculations [1,2]. The published calculations were performed at 100 kV with a sampling cell size of 128×128 and a slice thickness of 0.314 nm. It is well known that multislice is only valid:

(a) if the reciprocal space sampling is large enough, typically with the minimum dimension of the reciprocal space sampling cell being at least 60 nm^{-1}, the exact number depending on the algorithm used to avoid aliasing, the accelerating voltage and the atomic number of the atoms [#1];

(b) if the slice thickness is small enough, a typical number being less than 0.2 nm.

[#1] The number of beams in a multislice calculation is often quoted instead of the sampling. Since the sampling in reciprocal space depends upon the cell size whereas the number of beams used does not, the former is more significant.

Unfortunately multislice calculations seem to behave more like Fourier series than Taylor series, and if done improperly can lead to results such as spurious intensity oscillations. The standard validity test is to use smaller slices and a larger reciprocal space sampling to test that the calculations have converged. Since the unit cell size of the Si(111)7 × 7 reconstruction is about 2.6 nm, a 128 × 128 cell gives sampling at best to about 20 nm^{-1}. For reference, fig. 1 shows the amplitude of the (0, 0), ($\frac{1}{7}$, 1) and (0, $\frac{8}{7}$) surface spots for a validity check of the results on the zone axis. A cell size of 512 × 512 with a slice thickness of 0.157 nm is required for full convergence of the multislice calculations – results with half occupancy in each slice and a slice thickness of 0.157/2 nm lie on top of those for a 0.157 nm slice thickness within single precision numerical

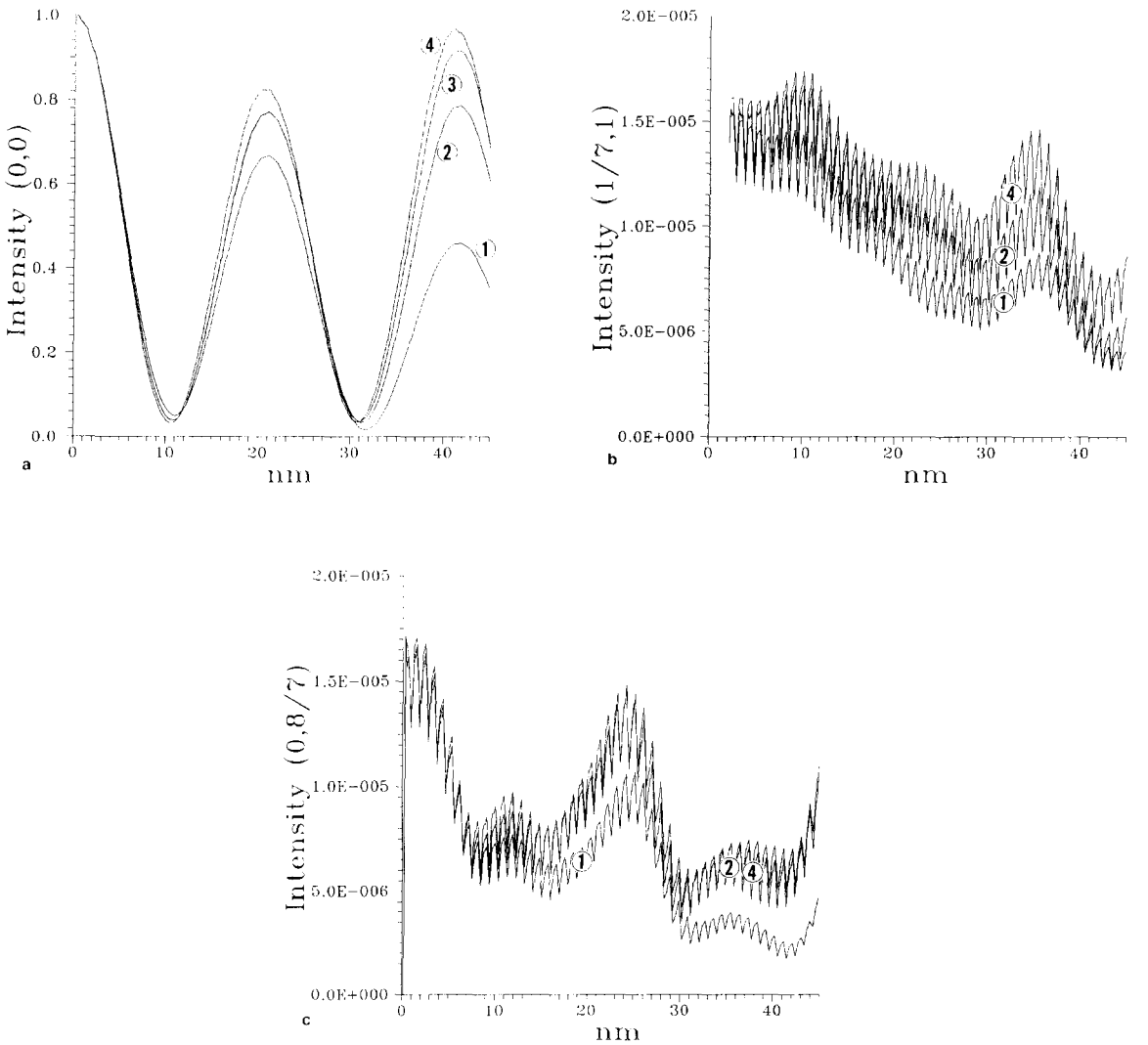

Fig. 1. Convergence tests for the Si(111)7×7 surface on the zone axis. In the graphs, 1 stands for 128×128 cell with 0.315 nm slice, 2 for a 256×256 cell with the same slice, 3 for a 512×512 cell with the same slice, and 4 for a 512×512 cell with 0.157 nm slice. Shown in (a) is the (0,0) intensity as a function of thickness, and in (b) the ($\frac{1}{7}$, 1) and (c) the (0, $\frac{8}{7}$) where (*hk*) is taken with using the surface 1×1 mesh.

error for the thickness regime investigated. (The data for the 128 × 128 cell will not match those previously published [1,2] since the results are very sensitive to the anti-aliasing algorithm used.) It should be mentioned that the programs used have been cross-checked against Bloch wave calculations and give identical results [5]. The difference is far smaller with a calculation off the zone axis (since the scattering is weaker), and a 128 × 128 calculation appears to be reasonable under these conditions as shown in fig. 2.

There therefore exists the possibility that the conclusion concerning a kinematical interpretation, which to date has been based solely upon multislice calculations, might be incorrect. The intention of this note is to provide, briefly, experimental verification of an essentially kinematical interpretation of surface diffraction using the

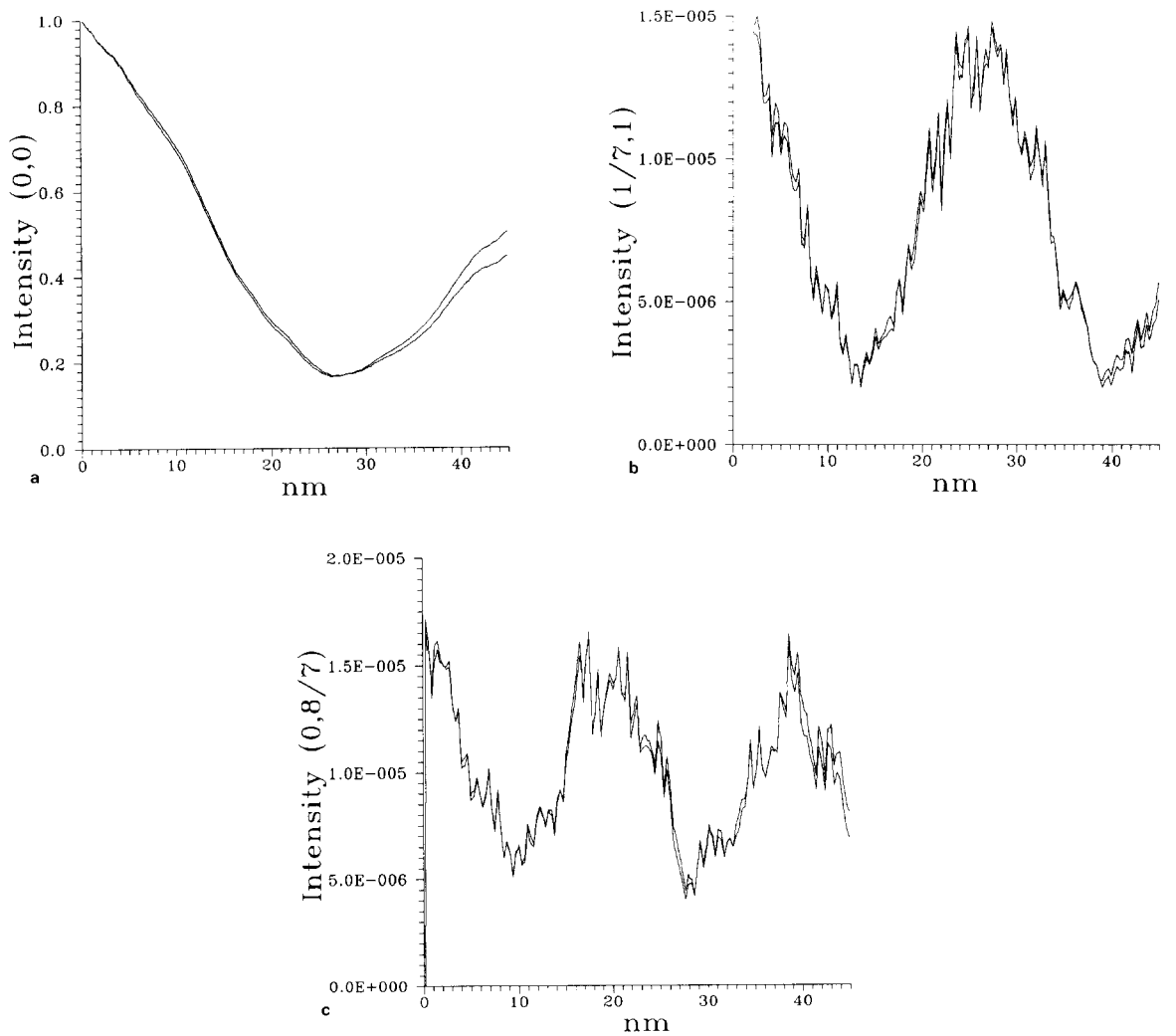

Fig. 2. Convergence tests for the Si(111)7×7 surface with the center of the Laue circle at (5.48, 4.67), comparing the result with a 128×128 cell with 0.315 nm slice and a 512×512 with 0.157 nm slice. In both cases the lower intensities are for the 128×128 sampling.

boron-doped Si(111) $\sqrt{3} \times \sqrt{3}$ R30° surface using the fact that for this surface the $(\frac{2}{3}, \frac{2}{3})$ spots are kinematically weak and dynamically can be strong.

2. Experimental method

Details of the UHV microscope used are described elsewhere [6,7] and will not be repeated here. We will also focus on the kinematical issue, not dealing substantially with other features of the surface which will also be discussed elsewhere.

Boron-doped silicon (111) samples were prepared via standard electron microscopy techniques as electron-transparent samples. After loading into the side chamber of the microscope [6,7], they were carefully ion-beam-cleaned to remove carbon and then annealed at about 800°C for 5 min.

3. Results and analysis

Fig. 3 shows electron diffraction patterns of the reconstructed surface in (a) along the [111] zone axis and in (b) tilted off to a pseudo-kinematical condition. The structure of this particular surface is well established [8–11], and corresponds to the substitution of a boron atom for a silicon atom in the second layer with a silicon adatom sitting on top in a $\sqrt{3} \times \sqrt{3}$ lattice rotated by 30° with respect to the 1×1 surface, and a contraction of the boron–silicon bond lengths relative to Si–Si in the top layer as sketched in fig. 4. The important result is the intensity of the $\{\frac{2}{3}, \frac{2}{3}\}$ surface diffraction spots (arrows) and the $\{\frac{4}{3}, \frac{2}{3}\}$ in the two cases as marked. Kinematically, the first of these is weak and the second strong, as indicated by the listing of selected values of $|F_{hk}|^2$ in table 1, a direct consequence of the in-plane boron–silicon contraction. Therefore the $\{\frac{2}{3}, \frac{2}{3}\}$ intensities is a classic example of a weak kinematical spot that can become strong dynamically, and fig. 3b can therefore be taken as an experimental demonstration that the intensities are kinematical in character. (We have performed

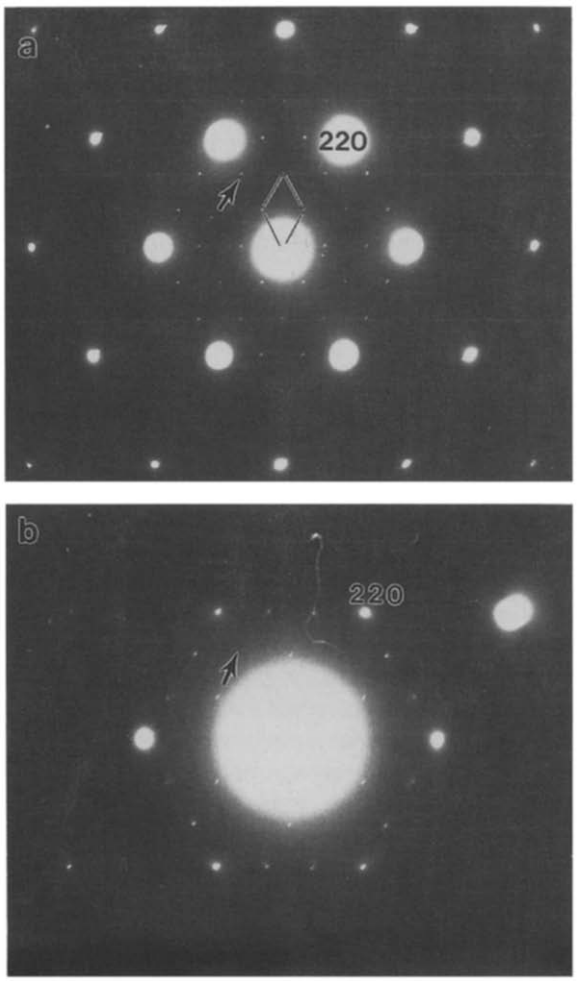

Fig. 3. Experimental images of the boron-doped Si(111) $\sqrt{3} \times \sqrt{3}$ R30° surface in (a) along the [111] zone axis, and in (b) tilted off to a pseudo-kinematical condition. The unit cell of the reconstruction is indicated in (a).

Table 1
Values of $|F_{hk}|^2$ for some of the reflections from the first surface layer for the Si(111) $\sqrt{3} \times \sqrt{3}$ R30° boron-doped surface using the 1×1 surface mesh; note that the (11) reflection is the same as a bulk {220}, and that the (10) corresponds to the unreconstructed 1×1 surface spot

h	k	$\lvert F_{hk} \rvert^2$
1/3	1/3	20.25
2/3	2/3	0.26
1	0	20.25
1	1	121.22
4/3	2/3	121.67
5/3	2/3	5.83
4/3	4/3	8.31

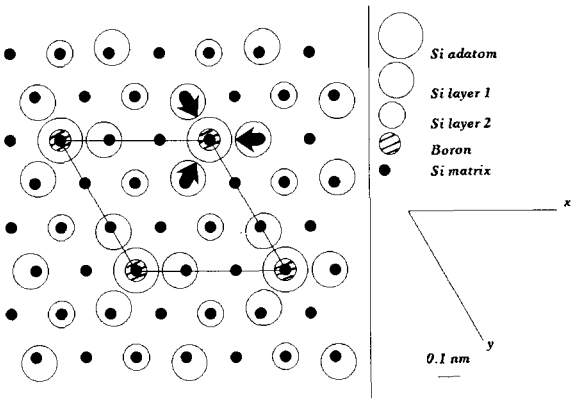

Fig. 4. Structure of the boron-doped Si(111)$\sqrt{3} \times \sqrt{3}$ R30° surface showing the in-plane change in position of the silicon atoms around the boron, indicated by the arrows.

multislice calculations to confirm that this feature does appear in the simulations, but an experimental proof would appear to be stronger.)

4. Discussion

The fact that a kinematical bulk diffraction condition can be used to generate essentially kinematical surface diffraction would appear to be correct. Obviously there are pitfalls in multislice simulations, but it is worth mentioning that the multislice method appears to be rigorous although inelastic scattering needs to be included for surfaces [12]. So long as one is using multislice to simulate diffraction patterns or amplitude contrast bright-field/dark-field inelastic scattering can, of course, be included via an optical potential approach. Unfortunately, it is still unclear whether this is valid for high resolution since one has to worry that much of the inelastic signal is included in the final image.

5. Conclusion

The kinematical interpretation of surface diffraction intensities off the zone axis is shown, experimentally, to be valid.

Acknowledgements

This work was supported by the Airforce Office of Scientific Research on grant number AFOSR 86-0344 DEF. Funding for the UHV microscope was provided by the Keck Foundation, the National Science Foundation and the Airforce Office of Scientific Research, and would have been impossible without the efforts of Robbie Kosak.

References

[1] J.C.H. Spence, Ultramicroscopy 11 (1983) 117.
[2] Y. Tanishiro and K. Takayanagi, Ultramicroscopy 27 (1989) 1.
[3] K. Takayanagi, Y. Tanishiro, M. Takahashi and S. Takahashi, J. Vac. Sci. Technol. A 3 (1985) 1502.
[4] K. Takayanagi, Y. Tanishiro, S. Takahashi and M. Takahashi, Surf. Sci. 164 (1985) 367.
[5] Y. Ma and L.D. Marks, Acta Cryst. A 46 (1990) 11.
[6] J.E. Bonevich and L.D. Marks, J. Electron Microscopy Tech. (1989) in press.
[7] L.D. Marks, R. Ai, J.E. Bonevich, M.I. Buckett, D. Dunn, J.P. Zhang, M. Jacoby and P.C. Stair, Ultramicroscopy 37 (1991) 90.
[8] P. Bedrossian, R.D. Meade, K. Mortensen, D.M. Chen, J.A. Golovchenko and D. Vanderbilt, Phys. Rev. Lett. 63 (1989) 1257.
[9] R.L. Headrick, I.K. Robsinson, E. Vlieg and L.C. Feldman, Phys. Rev. Lett. 63 (1989) 1253.
[10] I.W. Lyo, E. Kaxiras and Ph. Avouris, Phys. Rev. Lett. 63 (1989) 1261.
[11] J.H. Huang and S.Y. Tong, Phys. Rev. B 41 (1990) 3276.
[12] L.D. Marks, Ultramicroscopy 38 (1991) 325.